Multilevel Tower Observations of Vertical Eddy Diffusivity and Mixing Length in the Tropical Cyclone Boundary Layer during Landfalls

JIE TANG

Shanghai Typhoon Institute, CMA, Shanghai, China

JUN A. ZHANG

NOAA/Atlantic Oceanographic and Meteorological Laboratory/Hurricane Research Division, and Cooperative Institute for Marine and Atmospheric Studies, University of Miami, Miami, Florida

SIM D. ABERSON AND FRANK D. MARKS

NOAA/Atlantic Oceanographic and Meteorological Laboratory/Hurricane Research Division, Miami, Florida

XIAOTU LEI

Shanghai Typhoon Institute, CMA, Shanghai, China

(Manuscript received 23 November 2017, in final form 21 June 2018)

ABSTRACT

This study analyzes the fast-response (20 Hz) wind data collected by a multilevel tower during the landfalls of Tropical Storm Lionrock (1006), Typhoon Fanapi (1011), and Typhoon Megi (1015) in 2010. Turbulent momentum fluxes are calculated using the standard eddy-correlation method. Vertical eddy diffusivity K_m and mixing length are estimated using the directly measured momentum fluxes and mean-wind profiles. It is found that the momentum flux increases with wind speed at all four levels. The eddy diffusivity calculated using the direct-flux method is compared to that using a theoretical method in which the vertical eddy diffusivity is formulated as a linear function of the friction velocity and height. It is found that below ~60 m, K_m can be approximately parameterized using this theoretical method, though this method overestimates K_m for higher altitude, indicating that the surface-layer depth is close to 60 m in the tropical cyclones studied here. It is also found that K_m at each level varies with wind direction during landfalls: K_m estimated based on observations with landward fetch is significantly larger than that estimated using data with seaward fetch. This result suggests that different parameterizations of K_m should be used in the boundary layer schemes of numerical models forecasting tropical cyclones over land versus over the ocean.

1. Introduction

Turbulent processes in the planetary boundary layer (PBL) regulate tropical cyclone (TC) intensity and structure based on theoretical and numerical studies (e.g., Emanuel 1995; Bryan 2012; Kepert 2012; Zhang and Marks 2015; Zhang et al. 2017; Bu et al. 2017). However, turbulence data in the PBL of TCs have been scarce because fixed or moving observational platforms do not survive the severe conditions in that region. Remote sensing observations, on the other hand, usually lack the temporal resolutions (>5 Hz) required for calculation of turbulent fluxes.

Turbulence measurements in the PBL over the ocean have been uniquely obtained by research aircraft with advanced turbulence sensors on board with sampling rates >20 Hz to resolve small-scale (<10 m) turbulent eddies. Aircraft observations of turbulent fluxes based on the direct method (i.e., eddy-correlation method) have been obtained in a limited number of TCs and mainly in regions with surface wind speed less than hurricane force (e.g., Moss 1978; Black et al. 2007). Zhang and Drennan (2012) analyzed collocated turbulent flux data and dropsonde-measured mean quantities to estimate the vertical eddy diffusivity in surface wind

Corresponding author: Dr. Jun Zhang, jun.zhang@noaa.gov

DOI: 10.1175/JAS-D-17-0353.1

© 2018 American Meteorological Society. For information regarding reuse of this content and general copyright information, consult the AMS Copyright Policy (www.ametsoc.org/PUBSReuseLicenses).

speeds ranging between 16 and 30 m s^{-1} and in the layer between 70- and 800-m altitude. They also compared their results to previous PBL flux parameterizations in theoretical and numerical studies.

Few eyewall penetrations have been made by research aircraft within the TC PBL. Although limited by the 1-Hz temporal resolution, flight-level data collected at ~500-m altitude in intense storms Hurricanes Allen (1980) and Hugo (1989) have provided the first estimates of vertical eddy diffusivity for surface wind speed >30 m s^{-1} (Zhang et al. 2011a). These observational data have also led to an improved PBL parameterization scheme in the operational Hurricane Weather Research and Forecasting Model (HWRF) thus improving intensity forecasts (Zhang et al. 2015, 2017). Besides the abovementioned in situ turbulence observations, Lorsolo et al. (2010) presented a novel technique to calculate turbulent kinetic energy (TKE) in hurricanes using Doppler radar measurements. They found that the largest TKE is located in the PBL of hurricane eyewalls.

Turbulence observations over land in TCs are as difficult to obtain as those over the ocean because of the severe environment for an instrument and data system to survive. Almost all the previously reported turbulence observations during landfalling TCs are from tower observations that have maximum height at or below 10-m altitude (e.g., Yu et al. 2008; Zhu et al. 2010; Zhang et al. 2011b). These observational studies point out that the magnitude of momentum flux over land is typically larger than that over the ocean likely because of the greater surface roughness. Zhang et al. (2011b) have found that the variance of the drag coefficient is much larger in low- to moderate- (<10 m s^{-1}) wind conditions than in high-wind conditions. They also found that the dissipative heating estimated from the turbulent spectra is much smaller than that calculated using theory, consistent with aircraft observations over the ocean given by Zhang (2010).

Kosiba and Wurman (2014) studied the PBL structure of landfalling Hurricane Frances (2004) using dual-Doppler radar data and estimated the TKE following the method of Lorsolo et al. (2010). Their observed TKE values are comparable to those reported by Lorsolo et al. (2010) in hurricanes over the open ocean. Kosiba and Wurman (2014) found that PBL roll-like structures enhance turbulent transport in the PBL during hurricane landfalls. The Doppler radar data with TKE estimates are usually limited to altitudes above 150 m.

Above all, very little is known about vertical turbulent mixing processes in the PBL of TCs because of a lack of observation. Thus, the same PBL scheme used in simulations and forecasts over the ocean is typically used in those of landfalling TCs. Recently, Zhang and Pu (2017) found that using the same PBL scheme over land as over the ocean could cause problematic forecasts of TC intensity for landfalling hurricanes using HWRF forecasts. It is invaluable to provide reasonable estimates of vertical eddy diffusivity and mixing length using observations. This study is the first attempt to estimate these turbulence parameters using data collected by a multilevel tower during TC landfalls.

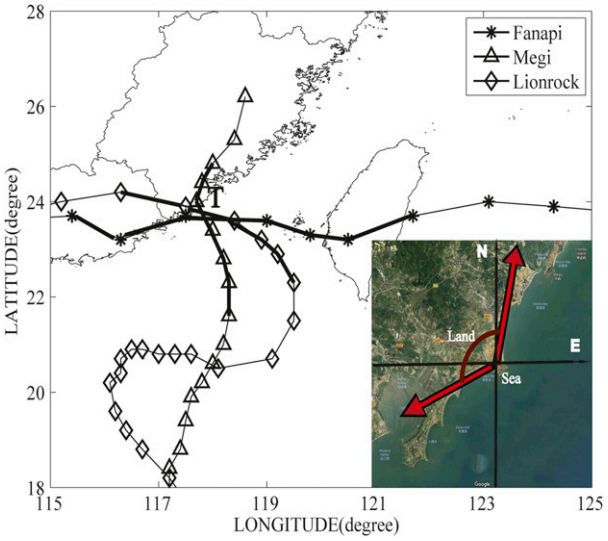

FIG. 1. Storm tracks of Tropical Storm Lionrock and Typhoons Fanapi, and Megi (2010). The location of Zhangpu tower is donated by letter "T." A plan-view photo of the tower is shown at the lower-right corner, with the red lines separating azimuths characteristic of land-dominated vs sea-dominated boundary layers.

2. Data and analysis method

In this study, data collected by a multilevel tower during landfalls of three TCs, [Tropical Storm Lionrock (1006), Typhoon Fanapi (1011), and Typhoon Megi (1015)] are analyzed. The tower was deployed by the Shanghai Typhoon Institute at Chihu, Zhangpu, of Fujian province in China (24.036°N, 117.897°E). The tower location and tracks of the three TCs are shown in Fig. 1. The tower was erected at an elevation of about 29 m and about 150 m away from the coastline. It was equipped with WindMaster Pro 3D supersonic anemometers, manufactured by British Grill, at four levels: 26.6, 42.4, 60.4, and 82.9 m above the ground. The data sampling rate of the three-dimensional wind velocity and virtual temperature is 20 Hz. After quality control, we selected a total of 147 flux runs,[1] and each flux run contains ~30 min of observations. Flux runs

[1] Here a flux run is defined as the period of data that are used for flux calculation.

are selected based on stationarity of the measurement following Zhang et al. (2009). The same method used by Tang et al. (2015) for data quality control is followed here. It should be noted that only flux runs with leg-average horizontal wind speed $>5\,\mathrm{m\,s^{-1}}$ are used in the final analysis as the emphasis of this study is on the flux and diffusion in strong wind conditions. Details of the field experiment and data description can be found in Tang et al. (2015).

Turbulent momentum flux τ is calculated using the traditional eddy-correlation method in the form of:

$$\hat{\tau} = \rho(-\overline{w'u'}\mathbf{i} - \overline{w'v'}\mathbf{j}), \tag{1}$$

where ρ is the air density; u, v, and w are the along-wind (**i**), crosswind (**j**), and vertical components of the wind velocity, respectively; the prime represents turbulent fluctuations; and the overbar is the time average during a 30-min leg. The linear trend in the data has been removed before averaging for turbulent fluctuations.

Based on standard K theory (Zhang et al. 2011a; Zhang and Drennan 2012), we calculate the vertical eddy diffusivity of momentum K_m as a function of the momentum flux and strain rate S using

$$K_m = |\tau| S^{-1}, \tag{2}$$

where S is defined as

$$S = \sqrt{\left(\frac{\partial \overline{u}}{\partial z}\right)^2 + \left(\frac{\partial \overline{v}}{\partial z}\right)^2}, \tag{3}$$

where the overbar represents averaging over the leg.

Here, we only use flux runs that have continuous wind and flux measurements at all four levels to make sure we get meaningful estimates of S or directional wind shear. The vertical mixing length l can be estimated using

$$l = \sqrt{\frac{K_m}{S}}. \tag{4}$$

In PBL schemes (e.g., Blackadar 1962; Louis 1979) used in numerical models where vertical turbulent fluxes are parameterized using K_m, l is usually calculated based on the asymptotic mixing length ℓ_∞ in the following form:

$$\frac{1}{\ell} = \frac{1}{\kappa z} + \frac{1}{\ell_\infty}, \tag{5}$$

where κ is the von Kármán constant and equals to 0.4, and z is the altitude. Thus, in addition to l, we can also estimate ℓ_∞ using the observational data in this study.

In the surface layer, surface wind stress can be related to the surface frictional velocity u_*, and K_m is usually parameterized using

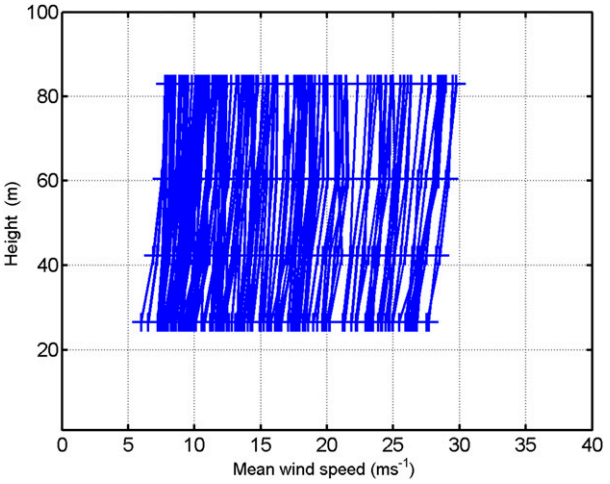

FIG. 2. Mean wind speed as a function of height in logarithmic scale for all the flux runs that have measurements at all four levels.

$$K_m = \kappa u_* z \phi, \tag{6}$$

where u_* is the frictional velocity and $u_* = \sqrt{|\tau|}$, ϕ is the stability function that is calculated using the Monin–Obukhov length L that is determined as follows:

$$L = -\frac{u_*^3 T_v}{kg\overline{T_v' w'}}, \tag{7}$$

where T_v is the virtual temperature. Of note, Katz and Zhu (2017) pointed out that L can be determined using the mean winds from different levels through an iteration method. Here we use the direct method to calculate L as T_v is measured by the sonic anemometers that provide the wind data. By comparing the estimated K_m based on the direct-flux method, as in Eq. (2) and the theoretical method as in Eq. (6), we can approximately evaluate if the observations are taken within or above the surface layer.

3. Results

Vertical profiles of the mean wind speed from the quality-controlled flux runs are shown in Fig. 2. Among all of these flux runs at all four vertical levels, the maximum 30-min averaged wind speed is $29.76\,\mathrm{m\,s^{-1}}$, which is close to hurricane force (i.e., $33\,\mathrm{m\,s^{-1}}$). Previous tower observations in hurricanes at altitudes at and below 10 m also reported flux data for wind speeds only up to similar maximum wind speed ($\sim 30\,\mathrm{m\,s^{-1}}$, e.g., Zhang et al. 2011b). It is evident from Fig. 2 that there is an increase of the wind speed with height for all the flux runs. In general, the wind speed has a logarithmic relationship with height as indicated by the nearly linear relationship

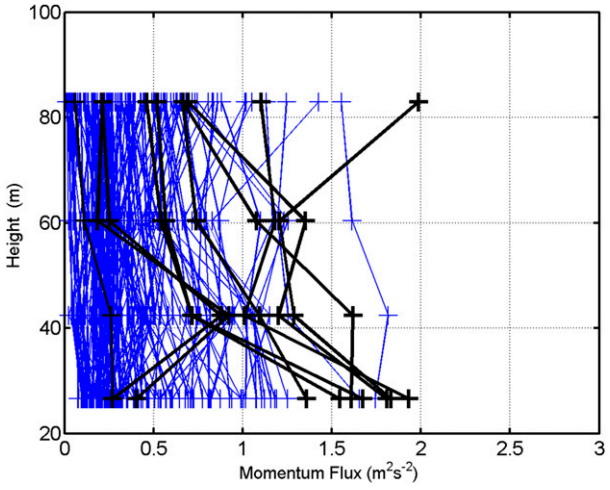

FIG. 3. Momentum flux as a function of altitude. Blue lines represent flux runs that have momentum flux independent with height, while black lines represent flux runs that have momentum flux varying with height.

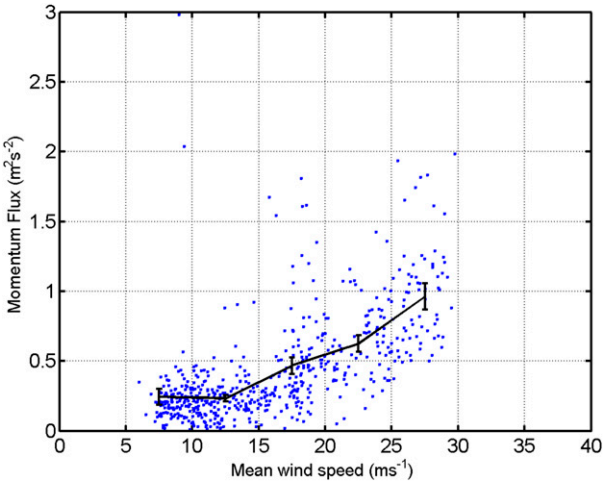

FIG. 4. Momentum flux as a function of wind speed at all altitudes. Solid vertical black lines show the 95% confidence interval within the wind speed range for bin average.

between the wind speed and log height. This result is consistent with wind profiles observed in a typical PBL in TCs (e.g., Powell et al. 2003; Ming et al. 2015). The small deviation of the vertical wind profile from the logarithmic relationship is mainly due to the stability effect according to Monin–Obukhov similarity theory of the surface layer (Monin and Obukhov 1954).

Momentum fluxes computed based on Eq. (1) for all the flux runs are shown in Fig. 3 as a function of height. It is evident that the momentum flux is nearly constant with height for the majority of the flux runs as indicated by the blue lines in Fig. 3. There is a weak trend of decrease of the momentum flux with height for these flux runs but this slope is not statistically significant. Interestingly, ~15% of the vertical profiles of the momentum fluxes show relatively large variations with height (black lines in Fig. 3), and most of these profiles show the decrease of the momentum flux with height with a nonzero slope. Given that the atmospheric surface is defined as the layer where turbulent fluxes are constant (Stull 1988), our result indicates that the top of the surface layer in the typhoons we studied here is mostly below ~80-m altitude. Previous aircraft studies presented vertical profiles of momentum fluxes in the low-level boundary layer (<500 m) and typically showed a linear decrease of the momentum flux with height (e.g., Moss 1978; Nicholls and Readings 1979; Grant 1992; French et al. 2007; Zhang et al. 2009). At the bottom of the boundary layer close to the surface, they usually found that momentum fluxes are nearly constant with height, which is similar to the tower observations in our study.

The momentum flux as a function of the mean wind speed for each flux run is shown in Fig. 4, indicating an increasing trend of the momentum flux with the wind speed up to the maximum wind speed measured by the tower. This result is consistent with previous studies that reported momentum flux measurements in moderate wind conditions ($<15\,m\,s^{-1}$) both over land and ocean (e.g., Mahrt 2000; Donelan et al. 1997; Banner et al. 1999; Fairall et al. 2003; French et al. 2007; Zhang et al. 2011b; Potter et al. 2015). From Fig. 4, the momentum flux in tropical storm–force or stronger wind speeds ($>18\,m\,s^{-1}$) is about 2–3 times that in lower wind speeds ($<10\,m\,s^{-1}$). The magnitude of the momentum flux within the wind speed range of 16–30 $m\,s^{-1}$ is on the order of 0.5–2 $m^2\,s^{-2}$, which is larger than that observed over ocean in similar wind speed conditions (French et al. 2007; Potter et al. 2015). This is likely due to the larger surface roughness over the area of tower observation than that over the open ocean as in previous studies. Figure 4 also suggests that the wind speed dependence of momentum flux is weaker for wind speeds $<18\,m\,s^{-1}$ than for larger wind speeds.

The strain rate S is shown as a function of altitude in Fig. 5. It is encouraging to see that the values of S are comparable to those reported by Zhang and Drennan (2012) based on analyses of in situ aircraft turbulence observations. It is evident from Fig. 5 that S decreases with height from 26. 6 to 60.4 m, and then either remains constant or slightly increases with height above 60.4 m. The S structure is similar to that given by Zhang and Drennan (2012), except that they found S to decrease with height up to 200 m instead of ~60 m before becoming nearly constant with height (see their Fig. 3a).

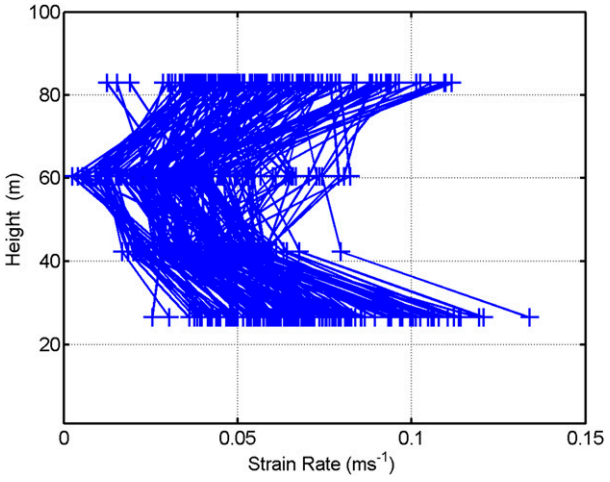

FIG. 5. Strain rate as a function of height for all the flux runs. Here the strain rate is calculated using Eq. (2).

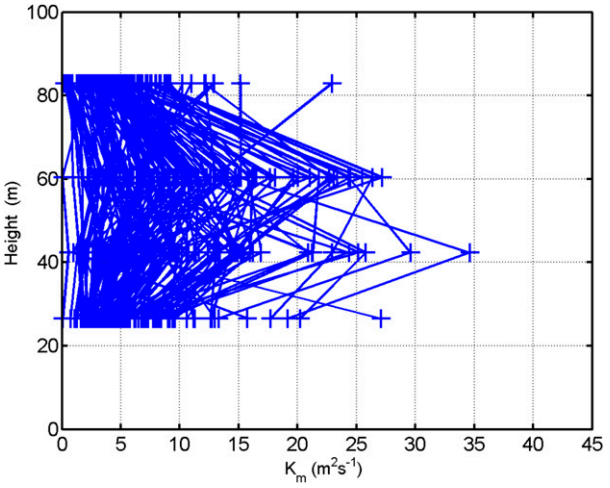

FIG. 7. Vertical eddy diffusivity K_m as a function altitude for all the flux runs.

Of note, their momentum fluxes are nearly constant with height below 200 m, suggesting a surface-layer height of ~200 m over the open ocean in the hurricanes they studied (see their Fig. 6a). This result suggests that the slope change of S with height may be an indicator for detecting the top of the surface layer. In the typhoons we studied here, the surface-layer depth is thus close to 60 m based on the above hypothesis. Furthermore, similar to the behavior of the momentum flux, S is found to increase with the wind speed (Fig. 6). The bin-averaged values of S show a near linear relationship with the wind speed. This result indicates that although there is substantial change in the vertical variation of S, the change in S with the wind speed at each vertical level is similar.

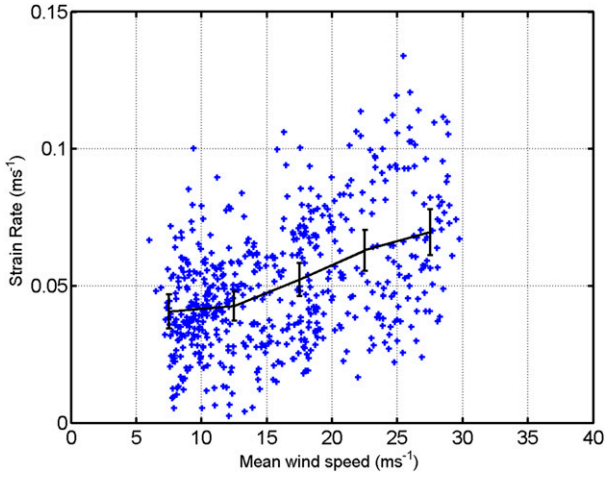

FIG. 6. Strain rate as a function of the mean wind speed. Solid vertical black lines represent the 95% confidence interval within the wind speed range for bin average.

The vertical eddy diffusivity for momentum K_m is calculated based on Eq. (2) and is presented in Fig. 7 as a function of height for all the flux runs. It is evident that K_m increases with height up to either 42.4 or 60.4 m and then decreases with height to 82.9 m. This behavior of K_m is similar to that given by Zhang and Drennan (2012) who also found an increase of K_m with height up to the top of the constant flux layer (~200 m in their case) before decreasing with height.

In the surface layer, it is expected to see that K_m increases with height as predicted by the Monin–Obukhov similarity theory [i.e., Eq. (4)]. When calculating u_*, we linearly extrapolate the momentum flux to 10-m altitude. Figure 8 shows u_* as a function of the wind speed, which essentially follows a similar trend in a similar manner as the momentum flux as shown earlier (cf. Fig. 4). This is expected because u_* is essentially the square root of the momentum flux at a given height, if there is no significant difference in the momentum flux at different levels. Figure 9 shows the eddy diffusivity calculated using the theoretical method ($\kappa u_* z \phi$) as a function of height and indicates a nearly linear increase with height up to 82.9 m. Here, the deviation of each vertical profile of the vertical eddy diffusivity from the linear trend is mainly due to the stability effect.

Figure 10 compares K_m calculated from the direct and theoretical methods, indicating that the theoretical method overestimates K_m for the majority of the flux runs at altitudes above 60.4 m. For flux runs with altitudes at 60.4 m and below, K_m estimates from the two methods tend to match, again suggesting that the top of the surface layer is ~60 m in the TC cases studied here.

Plotting K_m estimated using the direct-flux method as a function of wind speed shows that K_m weakly increases

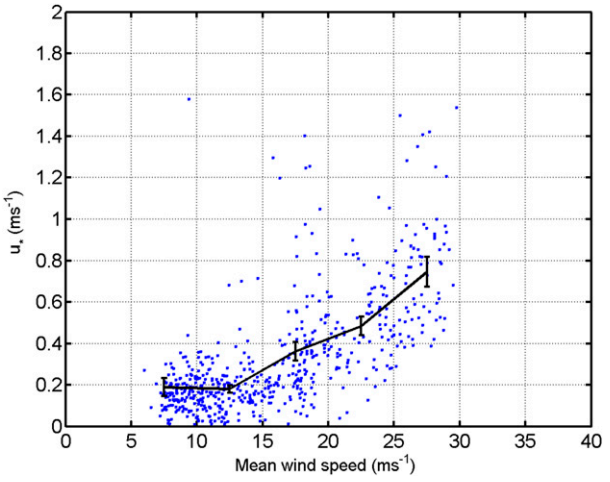

FIG. 8. Friction velocity u_* as a function of height. Solid vertical black lines represent the 95% confidence interval within the wind speed range for bin average.

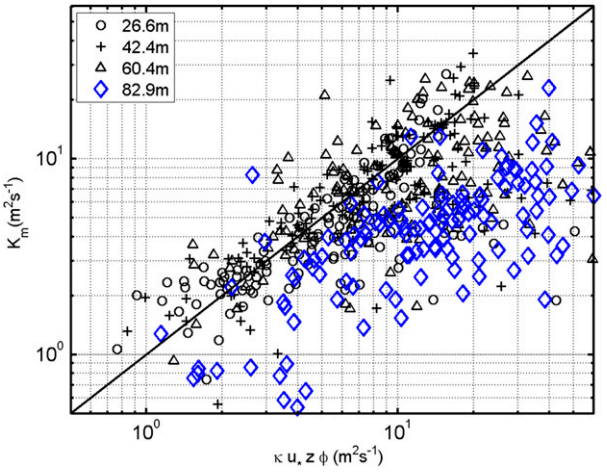

FIG. 10. Comparison of K_m calculated using the direct method and theoretical method ($ku_*z\phi$).

with wind speed (Fig. 11). The slope of the increase of K_m with wind speed is similar to that from Zhang and Drennan (2012). Zhang et al. (2011a) also found that K_m increases with wind speed at ~500-m altitude from moderate ($15\,m\,s^{-1}$) to much larger wind speeds ($>40\,m\,s^{-1}$) in the hurricane eyewalls of Hugo (1989) and Allen (1980).

Using the directly measured fluxes and K_m, we can also estimate the vertical mixing length and asymptotic mixing length following Eqs. (3) and (4). Figure 12a shows the histogram of the vertical mixing length for all altitudes, indicating that it ranges from 5 to 40 m with a near-normal distribution. The distribution of the asymptotic mixing length is slightly more skewed than that of the mixing length (Fig. 12b), with a median value of ~20 m and a maximum value of about 100 m. Zhang and Drennan (2012) found larger values of mixing length than we found here, likely because of larger wind speeds and higher observational altitude in their observations than those from our study. Furthermore, there is a weak increasing trend of the mixing length as a function of the wind speed (Fig. 13a), which is consistent with the result of Zhang and Drennan (2012). Although there is a weak dependence of the asymptotic mixing length on the wind speed (Fig. 13b), the increase in the asymptotic mixing length is not significant because of the large scatter.

It is well known that wind directions vary as storms approach or move away from a fixed observation station. During TC landfalls, when the observation station

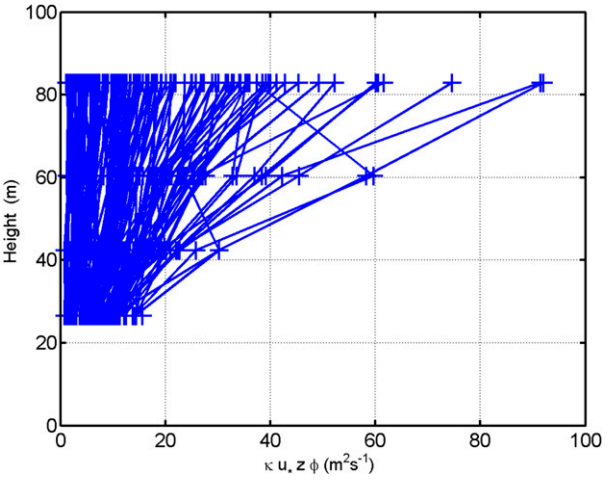

FIG. 9. Vertical eddy diffusivity calculated using the theoretical method ($ku_*z\phi$) as a function of height.

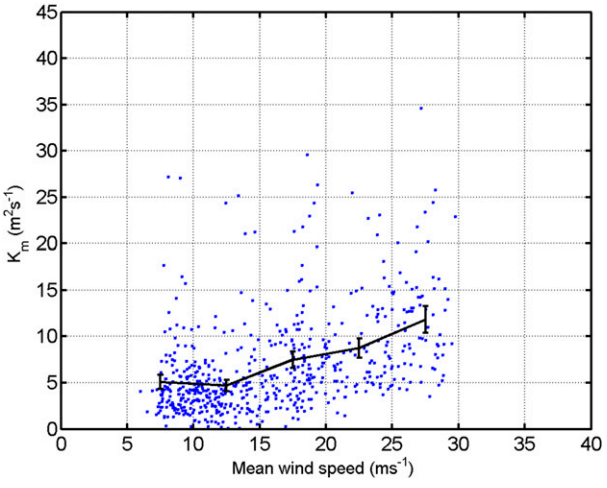

FIG. 11. Vertical eddy diffusivity K_m as a function of wind speed. Solid vertical black lines show the 95% confidence interval within the wind speed range for bin average.

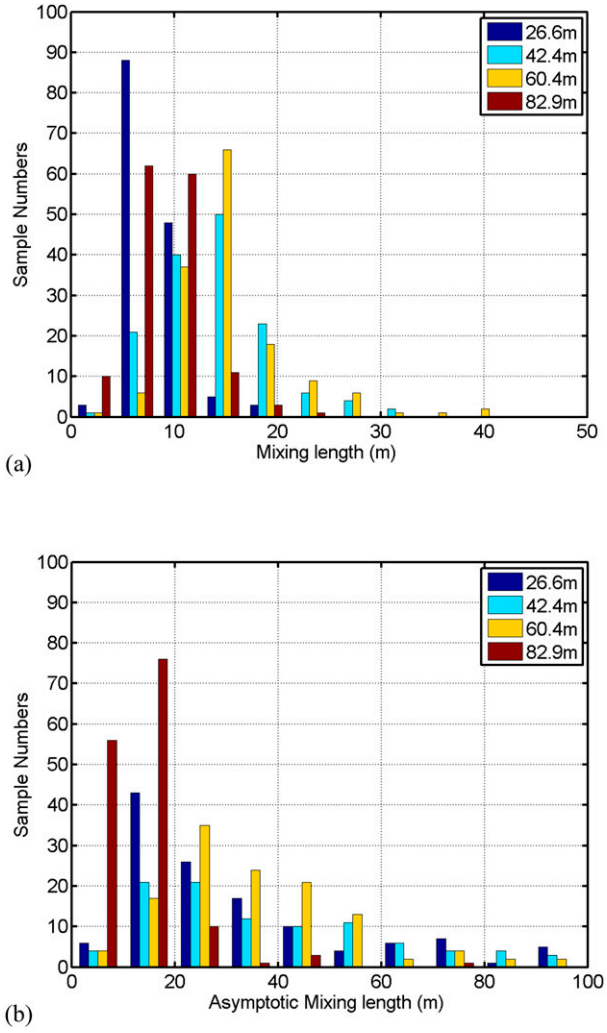

FIG. 12. Histogram of (top) vertical mixing length and (bottom) asymptotic mixing length. Each color represents the height of observation.

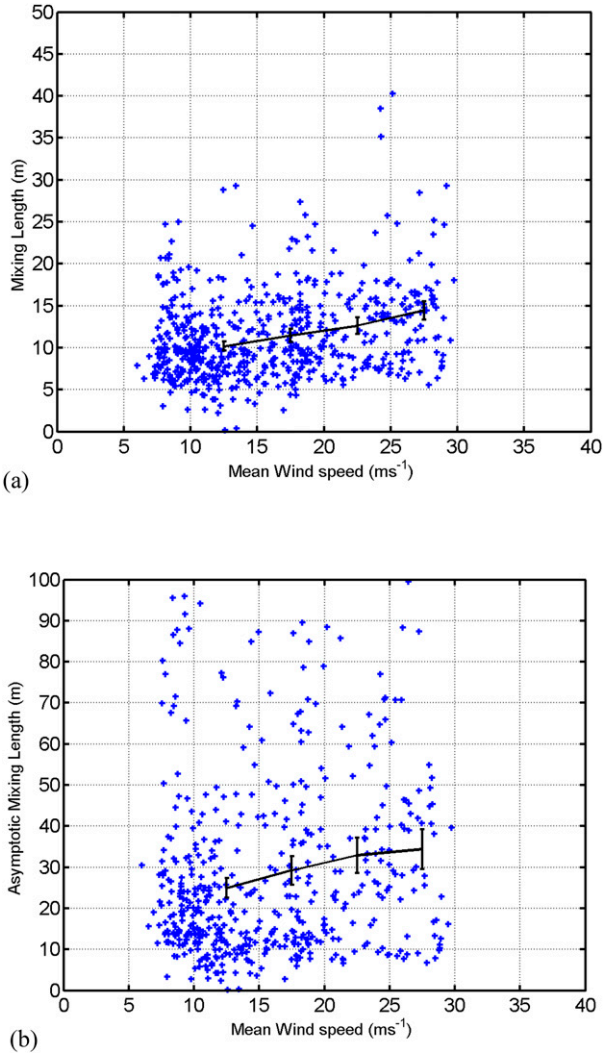

FIG. 13. (top) Vertical mixing length and (bottom) asymptotic mixing length as a function of the wind speed. Solid vertical black lines show the 95% confidence interval within the wind speed range for bin average.

such as the tower in our study is located at the coastline, changes in the wind direction are associated with changes in the types of the topography upstream of the tower (cf. Fig. 1). Figure 14 shows K_m based on the direct method as a function of wind direction using data 12 h before and after landfalls, indicating a near wavenumber-1 asymmetry of K_m with respect to the direction along the coastline. The values of K_m with landward fetch are found to be ~30% larger than those with seaward fetch at a given wind speed range (Fig. 15a). Similarly, the mixing length from flux runs with landward fetch is about 40%–50% larger than that with seaward fetch (Fig. 15b). Statistical analysis shows that the difference in both K_m and the mixing length between onshore and offshore flow is significant at the 95% confidence interval. This result thus suggests that variation of K_m and mixing length at a given wind speed is tied to the change in the effective surface roughness, which should be taken into account in numerical TC models.

4. Discussion and conclusions

Based on the data collected during the CBLAST experiment, a series of observational studies on the turbulent mixing in the PBL of hurricanes were conducted (e.g., French et al. 2007, Drennan et al. 2007; Zhang et al. 2009; Zhang and Drennan 2012). Most of these studies have focused on TCs over the open ocean. Very few studies investigating the landfall turbulent-mixing processes of TCs exist. As indicated by Zhang and Pu (2017), an understanding of the evolution of landfalling TCs in the

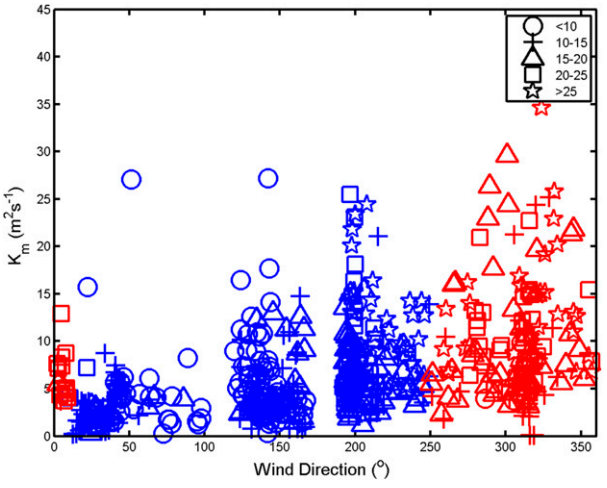

FIG. 14. Vertical eddy diffusion K_m as a function of the wind direction. Red represents the flux runs with wind direction from the land side, while blue represents the flux runs with wind direction from the ocean side. Each symbol represents a wind speed range.

context of turbulent mixing requires substantial work. Their study suggested that more accurate representation of vertical turbulent mixing in numerical model boundary layer schemes may help to comprehensively improve forecasts of TC wind decay and structure over land. To obtain more knowledge of turbulent processes during TC landfalls, we analyzed multilevel tower data to study the behavior of the vertical eddy diffusivity, momentum flux, and mixing length at wind speeds ranging between 5 and 30 m s^{-1}. This is the first observational study of eddy diffusivity for momentum transfer in the near-surface layer of TCs during their landfall stage.

Turbulent momentum fluxes were calculated using the standard eddy-correlation method. It is found also that the dependence of momentum flux on the wind speed is much smaller in weak-wind conditions (<18 m s^{-1}) than in tropical storm wind conditions (>18 m s^{-1}). There is a tendency for the momentum flux to increase with wind speed for wind speed >25 m s^{-1}.

Vertical eddy diffusivity and mixing length were first estimated using momentum fluxes and mean-wind profiles. It is found that the momentum flux increases with wind speed at all levels. The eddy diffusivity calculated using the direct method was then compared to that using the theoretical formulation as a function of friction velocity and height. It is found that below ~60 m, the eddy diffusivity estimated using these two methods matches well. The latter method overestimates K_m for altitudes higher than ~60 m, indicating that the surface-layer depth is close to 60 m in the landfalling TCs studied here. This surface-layer depth is much smaller than that over the open ocean at a similar wind speed regime given by Zhang and Drennan (2012).

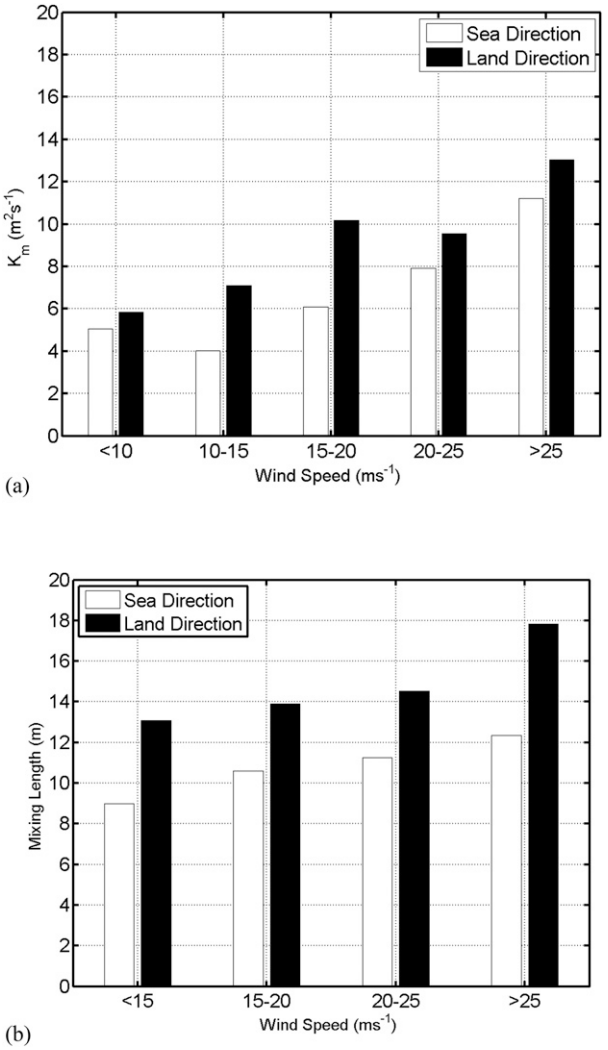

FIG. 15. Histograms of the (top) mean vertical eddy diffusion K_m and (bottom) mixing length separated by different wind directions at different wind speeds.

Comparison between observations from different wind directions close to the landfall time shows that the vertical eddy diffusivity and mixing length are significantly larger for flux runs that have winds blowing from land side than that from the ocean side. This difference should be considered in physical parameterizations of momentum fluxes through the eddy diffusivity and mixing length in numerical TC models. Our observational data support the finding of Zhang and Pu (2017) who suggested that the TC community should use different boundary layer parameterizations of vertical eddy diffusivity over land versus over ocean in TC simulations and forecasts.

It should be noted that the data utilized in this study are limited to the maximum wind speed of ~30 m s^{-1}. Future targeted field programs with advanced turbulence sensors on unmanned aircraft and buoys, or using

remote sensing techniques, are essential for fully understanding the turbulent-mixing and diffusion problems during TC landfalls.

Acknowledgments. This work was mainly completed during the first author's one-year visit at HRD under the Memorandum of Understanding between NOAA and CMA. Jie Tang and Xiaotu Lei were supported by the Key Program for International S&T Cooperation Projects of China (2017YFE0107700) and the National Natural Science Foundation of China (41475060, 41528501, and 41775065). The observational data in this study were from a field experiment supported by the Typhoon Scientific and Technological Innovation Group of the Shanghai Meteorological Service and the National Programme on Global Change and Air-Sea Interaction (GASI-IPOVAI-04) . Jun Zhang was in part supported by NOAA's Hurricane Forecast and Improvement Project (HFIP) with Award NA12NWS4680004 and NSF Grant AGS1822128. Sim Aberson and Frank Marks were supported by Hurricane Research Division base funding.

REFERENCES

Banner, M. L., W. Chen, E. J. Walsh, J. B. Jensen, S. Lee, and C. Fandry, 1999: The Southern Ocean Waves Experiment. Part I: Overview and mean results. *J. Phys. Oceanogr.*, **29**, 2130–2145, https://doi.org/10.1175/1520-0485(1999)029<2130:TSOWEP>2.0.CO;2.

Black, P. G., and Coauthors, 2007: Air–sea exchange in hurricanes: Synthesis of observations from the Coupled Boundary Layer Air–Sea Transfer Experiment. *Bull. Amer. Meteor. Soc.*, **88**, 357–374, https://doi.org/10.1175/BAMS-88-3-357.

Blackadar, A. K., 1962: The vertical distribution of wind and turbulent exchange in a neutral atmosphere. *J. Geophys. Res.*, **67**, 3095–3102, https://doi.org/10.1029/JZ067i008p03095.

Bryan, G. H., 2012: Effects of surface exchange coefficients and turbulence length scales on the intensity and structure of numerically simulated hurricanes. *Mon. Wea. Rev.*, **140**, 1125–1143, https://doi.org/10.1175/MWR-D-11-00231.1.

Bu, Y. P., R. G. Fovell, and K. L. Corbosiero, 2017: The influences of boundary layer vertical mixing and cloud-radiative forcing on tropical cyclone size. *J. Atmos. Sci.*, **74**, 1273–1292, https://doi.org/10.1175/JAS-D-16-0231.1.

Donelan, M. A., W. M. Drennan, and K. B. Katsaros, 1997: The air–sea momentum flux in conditions of wind sea and swell. *J. Phys. Oceanogr.*, **27**, 2087–2099, https://doi.org/10.1175/1520-0485(1997)027<2087:TASMFI>2.0.CO;2.

Drennan, W. M., J. A. Zhang, J. R. French, C. McCormick, and P. G. Black, 2007: Turbulent fluxes in the hurricane boundary layer. Part II: Latent heat flux. *J. Atmos. Sci.*, **64**, 1103–1115, https://doi.org/10.1175/JAS3889.1.

Emanuel, K. A., 1995: Sensitivity of tropical cyclones to surface exchange coefficients and a revised steady-state model incorporating eye dynamics. *J. Atmos. Sci.*, **52**, 3969–3976, https://doi.org/10.1175/1520-0469(1995)052<3969:SOTCTS>2.0.CO;2.

Fairall, C. W., E. F. Bradley, J. E. Hare, A. A. Grachev, and J. B. Edson, 2003: Bulk parameterization of air–sea fluxes: Updates and verification for the COARE algorithm. *J. Climate*, **16**, 571–591, https://doi.org/10.1175/1520-0442(2003)016<0571:BPOASF>2.0.CO;2.

French, J. R., W. M. Drennan, J. A. Zhang, and P. G. Black, 2007: Turbulent fluxes in the hurricane boundary layer. Part I: Momentum flux. *J. Atmos. Sci.*, **64**, 1089–1102, https://doi.org/10.1175/JAS3887.1.

Grant, A. L. M., 1992: The structure of turbulence in the near-neutral atmospheric boundary layer. *J. Atmos. Sci.*, **49**, 226–239, https://doi.org/10.1175/1520-0469(1992)049<0226:TSOTIT>2.0.CO;2.

Katz, J., and P. Zhu, 2017: Evaluation of surface layer flux parameterizations using in-situ observations. *Atmos. Res.*, **194**, 150–163, https://doi.org/10.1016/j.atmosres.2017.04.025.

Kepert, J. D., 2012: Choosing a boundary layer parameterization for tropical cyclone modeling. *Mon. Wea. Rev.*, **140**, 1427–1445, https://doi.org/10.1175/MWR-D-11-00217.1.

Kosiba, K. A., and J. Wurman, 2014: Finescale dual-Doppler analysis of hurricane boundary layer structures in Hurricane Frances (2004) at landfall. *Mon. Wea. Rev.*, **142**, 1874–1891, https://doi.org/10.1175/MWR-D-13-00178.1.

Lorsolo, S., J. A. Zhang, F. D. Marks, and J. Gamache, 2010: Estimation and mapping of hurricane turbulent energy using airborne Doppler measurements. *Mon. Wea. Rev.*, **138**, 3656–3670, https://doi.org/10.1175/2010MWR3183.1.

Louis, J. F., 1979: A parametric model of vertical eddy fluxes in the atmosphere. *Bound.-Layer Meteor.*, **17**, 187–202, https://doi.org/10.1007/BF00117978.

Mahrt, L., 2000: Surface heterogeneity and vertical structure of the boundary layer. *Bound.-Layer Meteor.*, **96**, 33–62, https://doi.org/10.1023/A:1002482332477.

Ming, J., J. A. Zhang, and R. F. Rogers, 2015: Typhoon kinematic and thermodynamic boundary layer structure from dropsonde composites. *J. Geophys. Res. Atmos.*, **120**, 3158–3172, https://doi.org/10.1002/2014JD022640.

Monin, A. S., and A. M. Obukhov, 1954: Basic laws of turbulent mixing in the surface layer of the atmosphere. *Tr. Geofiz. Inst., Akad. Nauk SSSR*, **24**, 163–187.

Moss, M. S., 1978: Low-level turbulence structure in the vicinity of a hurricane. *Mon. Wea. Rev.*, **106**, 841–849, https://doi.org/10.1175/1520-0493(1978)106<0841:LLTSIT>2.0.CO;2.

Nicholls, S., and C. J. Readings, 1979: Aircraft observations of the structure of the lower boundary layer over the sea. *Quart. J. Roy. Meteor. Soc.*, **105**, 785–802, https://doi.org/10.1002/qj.49710544604.

Potter, H., H. C. Graber, N. J. Williams, C. O. Collins, R. J. Ramos, and W. M. Drennan, 2015: In situ measurements of momentum fluxes in typhoons. *J. Atmos. Sci.*, **72**, 104–118, https://doi.org/10.1175/JAS-D-14-0025.1.

Powell, M. D., P. J. Vickery, and T. A. Reinhold, 2003: Reduced drag coefficient for high wind speeds in tropical cyclones. *Nature*, **422**, 279–283, https://doi.org/10.1038/nature01481.

Stull, R. B., 1988: *An Introduction to Boundary Layer Meteorology*. Atmospheric and Oceanographic Sciences Library, Vol. 13, Kluwer Academic, 670 pp., https://doi.org/10.1007/978-94-009-3027-8.

Tang, J., D. Byrne, J. A. Zhang, Y. Wang, X. Lei, D. Wu, P. Fang, and B. Zhao, 2015: Horizontal transition of turbulent cascade in the near-surface layer of tropical cyclones. *J. Atmos. Sci.*, **72**, 4915–4925, https://doi.org/10.1175/JAS-D-14-0373.1.

Yu, B., A. G. Chowdhury, and F. J. Masters, 2008: Hurricane wind power spectra, cospectra, and integral length scales. *Bound.-Layer Meteor.*, **129**, 411–430, https://doi.org/10.1007/s10546-008-9316-8.

Zhang, F., and Z. Pu, 2017: Effects of vertical eddy diffusivity parameterization on the evolution of landfalling hurricanes. *J. Atmos. Sci.*, **74**, 1879–1905, https://doi.org/10.1175/JAS-D-16-0214.1.

Zhang, J. A., 2010: Estimation of dissipative heating using low-level in situ aircraft observations in the hurricane boundary layer. *J. Atmos. Sci.*, **67**, 1853–1862, https://doi.org/10.1175/2010JAS3397.1.

——, and W. M. Drennan, 2012: An observational study of vertical eddy diffusivity in the hurricane boundary layer. *J. Atmos. Sci.*, **69**, 3223–3236, https://doi.org/10.1175/JAS-D-11-0348.1.

——, and F. D. Marks, 2015: Effects of horizontal eddy diffusivity on tropical cyclone intensity change and structure in idealized three-dimensional numerical simulations. *Mon. Wea. Rev.*, **143**, 3981–3995, https://doi.org/10.1175/MWR-D-14-00341.1.

——, W. M. Drennan, J. French, and P. G. Black, 2009: Turbulence structure of the hurricane boundary layer between the outer rainbands. *J. Atmos. Sci.*, **66**, 2455–2467, https://doi.org/10.1175/2009JAS2954.1.

——, F. D. Marks, M. T. Montgomery, and S. Lorsolo, 2011a: An estimation of turbulent characteristics in the low-level region of intense Hurricanes Allen (1980) and Hugo (1989). *Mon. Wea. Rev.*, **139**, 1447–1462, https://doi.org/10.1175/2010MWR3435.1.

——, P. Zhu, F. J. Masters, R. F. Rogers, and F. D. Marks, 2011b: On momentum transport and dissipative heating during hurricane landfalls. *J. Atmos. Sci.*, **68**, 1397–1404, https://doi.org/10.1175/JAS-D-10-05018.1.

——, D. S. Nolan, R. F. Rogers, and V. Tallapragada, 2015: Evaluating the impact of improvements in the boundary layer parameterization on hurricane intensity and structure forecasts in HWRF. *Mon. Wea. Rev.*, **143**, 3136–3155, https://doi.org/10.1175/MWR-D-14-00339.1.

——, R. F. Rogers, and V. Tallapragada, 2017: Impact of parameterized boundary layer structure on tropical cyclone rapid intensification forecasts in HWRF. *Mon. Wea. Rev.*, **145**, 1413–1426, https://doi.org/10.1175/MWR-D-16-0129.1.

Zhu, P., J. A. Zhang, and F. J. Masters, 2010: Wavelet analyses of turbulence in the hurricane surface layer during landfalls. *J. Atmos. Sci.*, **67**, 3793–3805, https://doi.org/10.1175/2010JAS3437.1.